



Improvement on Profile Path Reduction Factors for Rain Attenuation Predictions Using Vertically – Pointing Radar for Terrestrial and Satellite Applications in Tropical Region

J. S. Ojo^{1*}, M. A. Asaolu¹ and G. A. Ibitola²

¹*Department of Physics, Federal University Technology, Akure, Nigeria.*

²*Department of Physics, Ondo State University of Science and Technology, Okitipupa, Nigeria.*

Authors' contributions

This work was carried out in collaboration between all authors. Authors JSO and MAA designed the study, performed the statistical analysis, wrote the protocol, and wrote the first draft of the manuscript. Authors JSO and GAI managed the analyses of the study. Author GAI managed the literature searches. All authors read and approved the final manuscript.

Article Information

DOI: 10.9734/AIR/2018/40446

Editor(s):

(1) Martin Kröger, Professor, Computational Polymer Physics, Swiss Federal Institute of Technology (ETH Zürich), Switzerland.

Reviewers:

(1) P. Kasinatha Pandian, Karpaga Vinayaga College of Engineering and Technology, Anna University, India.

(2) Ionac Nicoleta, University of Bucharest, Romania.

(3) Işın Onur, Akdeniz University, Turkey.

Complete Peer review History: <http://www.sciencedomain.org/review-history/24116>

Original Research Article

Received 19th January 2018

Accepted 26th March 2018

Published 13th April 2018

ABSTRACT

More than ever before, applications of satellite services continue to gain recognition due to more growth in technological systems and applications. However, propagations along the Earth-space path suffer degradation due to hydrometeors such as rain, fog, haze, snow and hail. Among the hydrometeors, rain has been identified to be the most deterrent to satellite and terrestrial propagation links especially at frequency greater than 10 GHz. This paper proposes an improvement to effective path length for rain attenuation predictions in the tropic. Experimental data derived from vertically-pointing micro rain radar and Eutelsat 36B Ku-band link in Akure (Lat. 7° 25' E, Long. 5° 21' N), Southwestern Nigeria has been used. The proposed path length reduction model has been incorporated into the ITU-R model. The reduction factors were estimated for different rain types based on 5-year data (2012 - 2016). Comparison with the ITU model and some

*Corresponding author: E-mail: josnno@yahoo.com, ojojs_74@futa.edu.ng;

existing models indicate appreciably improve prediction accuracy for the location based on average percentage error and root mean square. The result will be applicable to communication systems operating at high elevation angles over the study location.

Keywords: Path reduction; micro rain radar; rain types; high elevation; tropics.

1. INTRODUCTION

The rapid development in communication systems has brought saturation to the lower frequency band ($f < 10$ GHz), consequently necessitating the exploration and utilisation of higher frequency spectrum in the millimetre waves region. It is not a gainsaying, that the advantages of higher frequency bands are innumerable; higher bandwidth, small antenna diameter and fast data rate to mention but few. However, at frequencies above 10 GHz, rain is the dominant contributed factor to signal degradation especially in tropical regions where convective rain type is dominant [1-4]. The amount of signal degradation along the earth to satellite paths become more severe as the frequency increases. Therefore, in designing microwave systems, the major problem in link design is to govern the excess attenuation due to rainfall. The importance of a radio link in a communication system makes the consideration and optimization of large number of specifications leading to signal degradation imperative. This is a bid to build an efficient communication system [5]. Frequency allocation is usually governed by national regulatory agencies in different countries such as Nigerian Communication Commission (NCC) in Nigeria under the umbrella of International Telecommunication Regulatory Union. Therefore the issue of attenuation, especially due to rain, is a compelling subject for research. This will enhance optimization of communication system through appropriate mitigation measures. In addition, the present study will also help in the link-budgeting design needed for migration to digital video satellite-broadcasting using high frequency bands.

The concept of rain attenuation in radio wave propagation is not new based on the several studies conducted both at the temperate and tropical regions [6-10]. The concept has been driven through measurement campaign and theoretical approaches [11]. Based on the several studies conducted, it has been established that the contributions of rain on signal degradation along Earth-space path is highly significant. Although measurement

campaign through satellite signal strength can provide good study for the subject matter, unfortunately, actual signal measurements in tropical environment are very limited [2]. Therefore, researchers have resorted into adoption of either semi-empirical or theoretical techniques to predict rain attenuation. In order to achieve this, adequate information on rainfall parameters must be known. Among the rainfall parameters, the rain height, rain rate, drop size distributions (DSD) and the propagation path length are the most common ones. Rain height can be deduced either through the latitudinal concept or melting layer techniques as recommended by the ITU-R 839-3 [12] and ITU-R 618-12 [13]. Both rain rate and drop sizes distribution can also be measured using rain gauge, Disdrometers and radar. In the case of propagation path length, the concept is included in the general rain attenuation prediction model recommended by the ITU based on point rainfall rate. The ITU-R model has been developed based data bank across the globe especially from the temperate region. It is therefore imperative to adopt the use of local data as input to the model. Rainfall rate is location dependent while precipitation along the propagation path is inhomogeneous both in the horizontal and vertical planes. Therefore, for communication systems using high elevation angles, appropriate approach that includes the local data to estimate attenuation due to rain is imperative. This can be achieved by adjusting the effective path length to account for the inhomogeneity of rain rate occurring along the propagation link. To achieve this concept experimentally is cumbersome, because associated links based on different propagation path lengths within the neighbourhood must be involved. Another method is to adopt the use of radar data to estimate attenuation due to inhomogeneity of rain for the simulated paths and based on different lengths [14]. The objective of this present work is to adopt a simple method to obtain rain attenuation statistics for tropical environments. An attempt is made to derive the effective path length along the vertical and horizontal paths. The result will be incorporated into existing rain attenuation model using power-law relations between the rain cell parameters

and radar reflectivity. The proposed model will be compared with the ITU model and some existing models.

The remaining portions of the paper are structured as follows: section two provides information on the experimental setup and data while section three gives information on the approach adopted. Section four is for results and discussion while section five gives the conclusive remarks.

2. SYSTEM DESCRIPTION AND DATA PROCUREMENTS

Since year 2007, the Communication Research Group of the Department of Physics, Federal University of Technology, Akure, (7.3043° N, 5.1370° E), has continuously measured vertical profile of rainfall parameters using vertically pointed Micro Rain Radar. For the purpose of this study, measurements between 2012 and 2016 will be analysed for the sake of uniformity based on measurement from the Ku-band satellite beacon. Generally, we have made use of the radar and Ku-band beacon measurements to achieve the objective of the present study.

The MRR used for the data collections employ the frequency modulated continuous wave (FM-CW) technique. It is capable of achieving time-series data based on smaller instantaneous transmitting powers and physical size. The transmitting power continuously emits periodic pulses whose frequency component is time dependent. The radar adopts both backscatter and Doppler spectrum techniques to give information on drop-size distribution and vertical velocity which transforms into rain intensity. The

DSD information is obtained by converting the measured Doppler spectra into drop diameters through a specified relationship [15]. Consequently, rain rates are measured indirectly by the radar based on the conversion of the radar reflectivity into rainfall rate. This could be achieved by initially solving the equation for R and converting the radar reflectivity z to reflectivity Z (dBZ) where Z is the reflectivity in dBZ. Meteorological radar is, therefore, a good tool to develop a rain-induced attenuation prediction model for both satellite and terrestrial microwave systems.

The radar indoor unit is located inside the Scintillation laboratory of the CRG unit while the outdoor unit is inside the observatory garden. The Doppler radar, operating at 24.1 GHz frequency, provides 160 m vertical sampling of precipitation from the surface up to 4800 m at integration time of 1 minute. The data were collected at 30 different range gates between 160 and 4800 meters above sea level in a stepwise of 160 m. During the measurement period, the accuracy of the radar data is around 91%. The remaining 9% outage period is due to system re-calibration and maintenance. Table 1 provides the specification for the radar system. A typing bucket rain gauge is also collocated with the MRR for ground-based measurements.

The Ku-band satellite beacon signal of frequency 12.245 GHz has also been continuously monitored from Eutelsat-36B (geostationary at longitude 36°E) with an elevation angle of 53.3° [16]. Eutelsat-36B is a Digital Video Broadcasting Satellite (DVB-S) that operates on both Multi Carrier Per Channel (MCPC) and Single Carrier Per Channel (SCPC) modes. The performance

Table 1. Specifications of the MRR

Radar Name	MRR
Radar Type	FM-CW
Location	FUTA
Position	7.3043° N, 5.1370° E, Elevation 325 m
Frequency (GHz)	24.1
Transmit Power (mW)	50
Receiver Type	Single polarization
Power Consumption (W)	50
Range Resolution (m)	160 – 4800
No of range gates	30
Antenna Type and Diameter (m)	Parabolic, 0.5
Beam width	1.5°

is based on Quadrature Phase Shift Keying (QPSK) modulation. The beacon satellite signal is received with an offset parabolic antenna of 0.9 m diameter with 40 dB gains. The horizontally polarized Ku-band satellite signal beacon is therefore down-converted to an L-band signal by using a low noise block converter (LNBC) having a noise figure of 0.5 db. The down converted signal is consequently fed into a Thrillithic Tektronix Y400 spectrum analyser. The video filtered output from the spectrum analyser is recorded and stored in a data logger before transferring into a computer.

3. METHODOLOGY

MRR operates on the principle of backscattering and Doppler spectrum techniques. This is achieved by emitting pulses toward specified meteorological targets. Some energy will be scattered back to the radar through the process. This phenomenon is referred to as backscattering. The backscattered power depends on some radar criteria, which are the number of the raindrops, the size, shape and dielectric constant [14]. Based on these criteria, we can estimate the radar reflectivity factor Z , and generate an empirical relationship between rain rate and Z .

Based on the report by Waldvogel, [17], Peter et al. [18] and Marzuki et al. [19] the integral parameters from the number of raindrops $N(D)$, can be expressed as:

$$R = \frac{6 \pi}{10^4} \int_0^{\infty} D^3 N(D) v(D) dD \quad (1)$$

while the radar reflectivity is related to the number of raindrops as:

$$Z = \int_0^{\infty} N(D) D^6 dD \quad (2)$$

where R is the rain rate in mm/h, Z is the radar reflectivity in dBZ

The empirical relationship exists between equations (1) and (2) through power law relations as [20]:

$$R = aZ^b \quad (3)$$

where Z is given in $\text{mm}^6 \text{m}^{-3}$, R in mmh^{-1} , a and b are coefficients which depend on the raindrop number distribution $N(D)$ as function of the drops diameter (D).

Equation (3) was used to determine the relationship between rainfall rate (R) and radar reflectivity factor (Z). Applying a natural logarithm on both sides of equation (3) resulting in:

$$\text{Ln } R = \text{Ln } a + b \text{ Ln } Z \quad (4)$$

The coefficients a and b of equation (4) were estimated by linear regression Z versus R .

The vertical profile of Z varies with height with different linear characteristics as [21]:

$$Z = a + b dh \quad (5)$$

The specific attenuation γ based on radar measurement can be expressed as:

$$\gamma = \alpha Z^\beta \quad (\text{dBkm}^{-1}) \quad (6)$$

The coefficients α and β are frequency dependent.

Hence, from (5) and (6) we have

$$\gamma_{(dh)} = \alpha(a + b dh)^\beta \quad (7)$$

Then $\gamma_{(dh)}$ at height h will be

$$\gamma_{(h)} = \alpha(10^{a/\beta/10} * 10^{hb/\beta/10}) \quad (8)$$

where $\alpha(10^{a/\beta/10})$ represents the specific attenuation at 160 m.

Formulation of the reduction factor from radar data for communications system at high elevation can be obtained based on the expression above.

Integrating equation (8) over vertical path length dh , and the specific attenuation at 160 m we obtained the attenuation $A_{dh}(p)$ not exceeded for time percentage's along dh .

Hence, the vertical reduction factor r_{vh} for a specified time percentage p , and rain height h is:

$$r_{vh}(p, dh) = \frac{A_{dh}(p)}{\gamma_{160}(p)L} \quad (9)$$

where γ_{160} is the specific attenuation at 160 m height (based on the present study) for the time percentage not exceeded as that of the attenuation and L is the total path length (km).

To derive the reduction factor r , we have restricted the vertical paths to the radar peak height of 4.8 km. Using the radar reflectivity in each rain gates, we have categorized rainfall rate to different rain types namely: stratiform and convective according to the specification in the work of Peter et al. [20].

Attenuation $A_{0.01}(p)$ for 0.01 % of the time for specified path lengths is first estimated for each of the rain types at the peak of the radar height. Thereafter, the total attenuation for each of the remaining paths is calculated for frequencies between 12 and 35 GHz to accommodate for the Ku and Ka-bands. Reduction factor r is then estimated from these calculations based on different rain types.

4. RESULTS AND DISCUSSION

Fig. 1(a and b) presents the attenuation values at 0.01% of time signal not available in a year based on the result at different frequency for each path for stratiform and convective rain types respectively. The attenuation values for 0.01% of the time for each path links of 1 to 4.8 km lengths; operating at 12, 16, 20, 30 and 35 GHz are extracted from the best-fit lines. The 0.01% has been chosen based on the fact that a good system must provide at least 99.99% reliability. Design and system engineers use this value to design communications system such that the link is available for a total time of 52.45 minutes for the specified year. Systems built with this value ensure reliable microwave link and guarantee customer satisfaction [22]. As usual, attenuation along the propagation path increases with

increase in frequency whereby convective rain type contributed mostly to the signal attenuation. The significant of these curves is that the ratio of attenuation exceeded for two different path lengths varies with frequency. For example, the ratio of attenuations between, 4 and 2 km paths should be equal to the ratio of the path lengths, i.e. 2. In fact, the ratio for these two distances increases to more than 5 for high frequencies associated with high rainfall rates and decreases for low frequencies associated with low rainfall rates. This implies that average rain cell diameters are smaller for the stratiform rain than for the more intense convective rain types. The results further show that as the path length increases, the amount of attenuation due to rain increase at a minimal rate. This is due to the fact that rain cells will not cover the whole path length at the same time.

Applying the plots presented in Fig. 1, the path reduction factor derived based on radar measurement at different frequencies can be deduced by simplifying equation (9). The resulted regression fit follows the power law relationship given as:

$$r_{0.01(160m)} = x * L^y + z \tag{10}$$

where x , y and z are constants obtained at each frequency. Fig. 2 (a-c) presents a typical plot of constant x , y and z against frequency respectively for the convective rain type while Table 2 presents the corresponding values for each frequency at different rain types. Based on

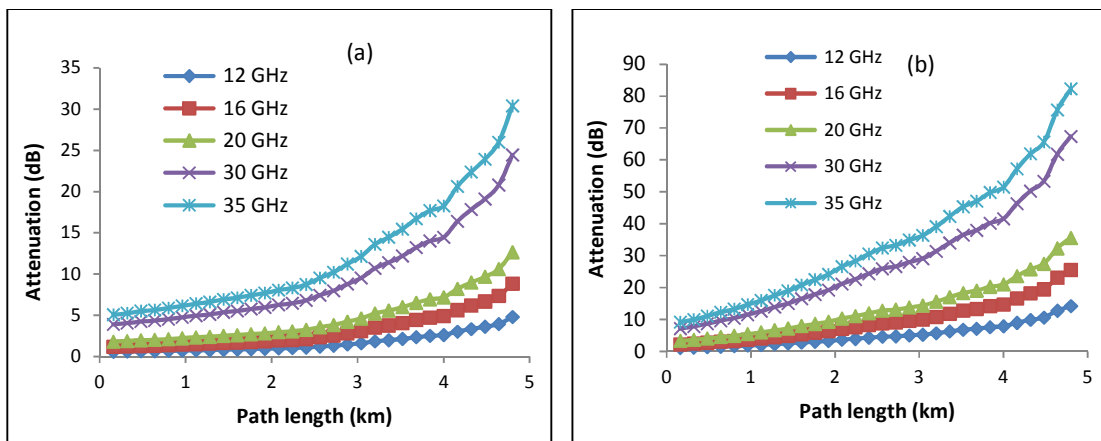


Fig. 1. Influence of attenuation values at 0.01% of time on path length at different frequency for (a) stratiform and (b) convective rain types

the plots in Figs 2 (a-c), the following expressions are generated as [11]:

$$x = 3.798 e^{\left[-\left(\frac{f-52.06}{23.34}\right)\right]} \quad (11)$$

$$y = -9260 f^{-7.585} - 0.6431 \quad (12)$$

$$z = 0.0007234 f^3 - 0.0345 f^2 - 0.0921 f + 0.234 \quad (13)$$

where f represents the frequency of operation in GHz.

Using equation (9), the values obtained in equation (10), and the values in Table 2, the reduction factors for path lengths of 1 to 4.8-km at selected frequencies are calculated. The

reduction factor values are plotted in Fig. 3 (a) and (b) for stratiform and convective rain type respectively.

In order to formulate proposed reduction factor model, a typical graph for worst case scenario at 35 GHz and for a convective rain type is presented in Fig. 4. From Figure 4 and based on curve fit line, the reduction factor can be formulated for a typical frequency-35 GHz as follows:

$$r_{0.01(160m)} = 0.448 * L^{-0.068} + 0.58 \quad (14)$$

where L is the path length in km. The same procedure is adopted for the other frequencies.

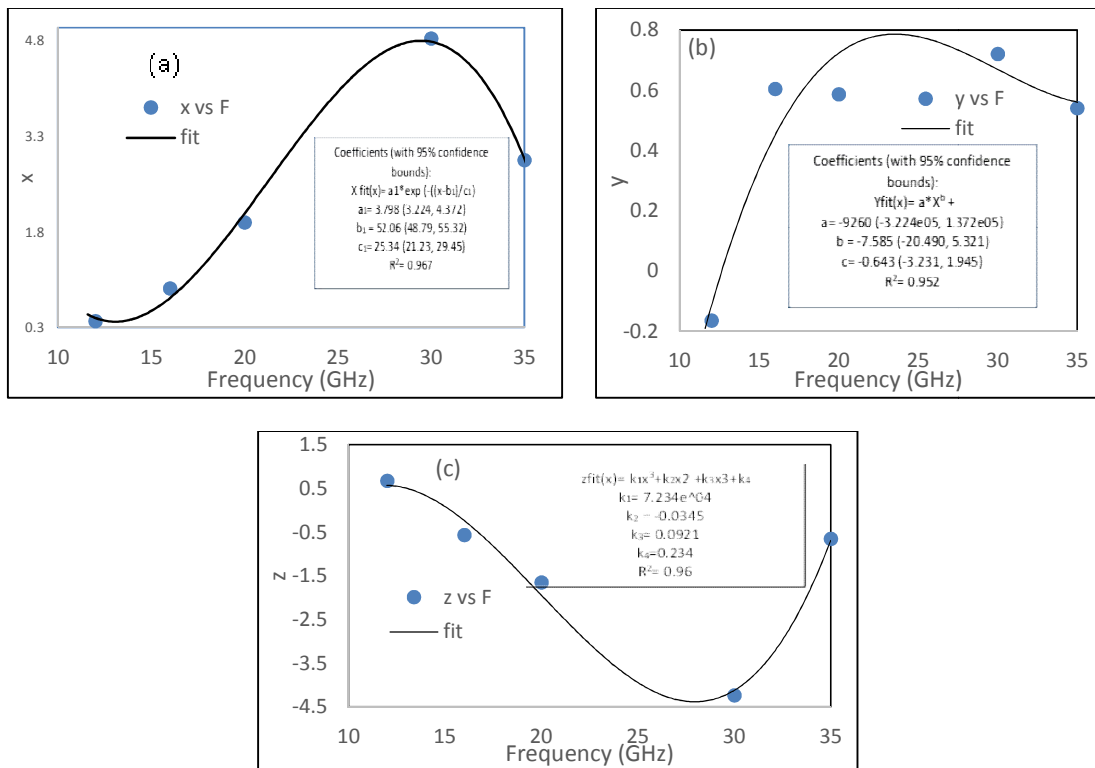


Fig. 2. Plots of constant (a) x , (b) y and (c) z against frequency in GHz.

Table 2. Constants for the line of best-fit for the reduction factor at different frequencies

Rain types	Stratiform rain types			Convective rain types		
Frequency (GHz)	x	y	z	x^*	y^*	z^*
12	0.346	-0.1651	0.5256	0.402	-0.1945	0.6745
16	0.856	0.6044	0.4567	0.914	0.6291	-0.5653
20	1.857	0.5868	0.0562	1.948	0.6025	-1.651
30	4.457	0.3208	-3.0510	4.831	0.3855	-4.2341
35	2.845	0.5406	-0.4351	2.925	0.5981	-0.6532

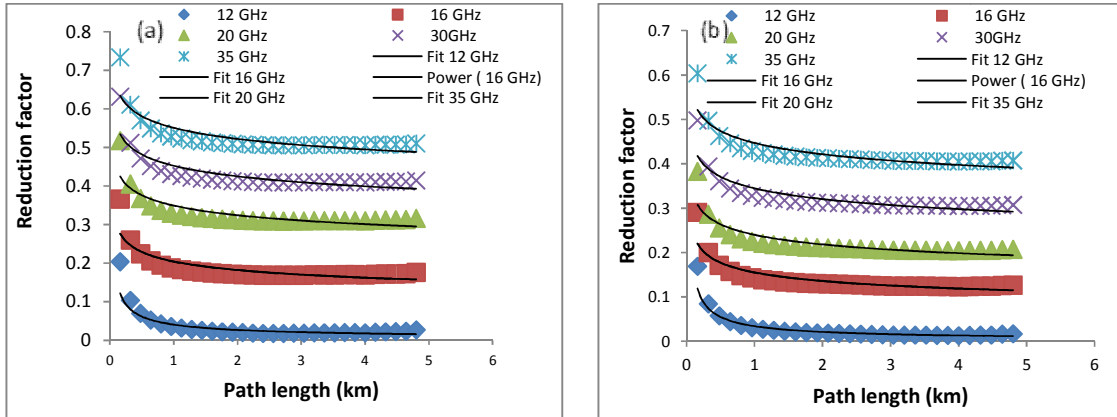


Fig. 3. Reduction factor (*r*) plots for 1 to 4.8-km path lengths at different frequencies for (a) stratiform and (b) convective rain types

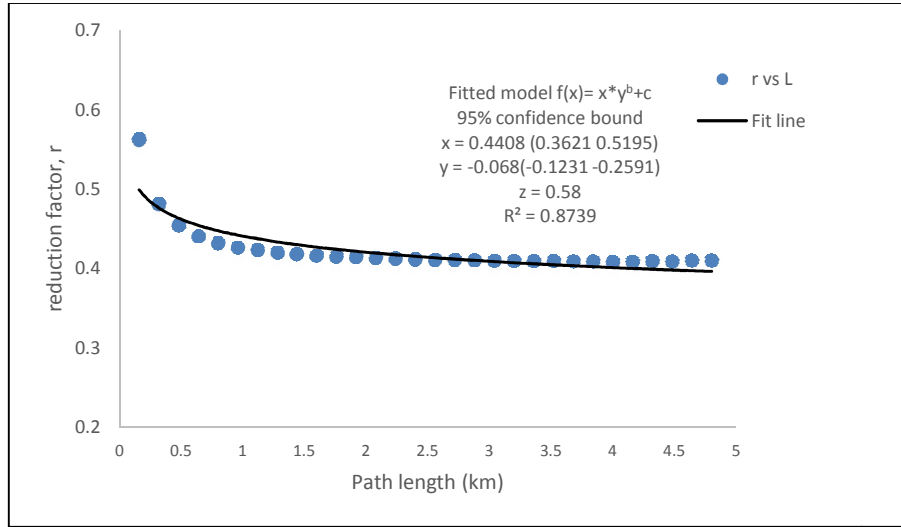


Fig. 4. Reduction factor (*r*) plots for 1 to 4.8-km path lengths at 35 GHz for 0.01% of the time

Five years experimental beacon data of rain attenuation are extracted from the archived data of Scintillation laboratory of the CRG unit, department of Physics, FUTA. Normalizing the effect of horizontal reduction factor from the rain-induced attenuation by using MATLAB tools result into a Gaussian law relationship as [11]:

$$F(x) = X_1 \exp \left[- \left(\frac{(\gamma_{R0.01} \cdot L_s)^{-1} - Y_1}{Z_1} \right)^2 \right] \quad (15)$$

where $F(x)$ is the vertical reduction factor (r_{vh}) and the coefficients X_1 , Y_1 and Z_1 are 1.628, 0.0423 and 0.02162 respectively.

Equations (14) and (15) are incorporated into steps 6 and 7 of the ITU-R 618-12 [13]. Details are not re-iterated here due to paucity of space, but they are readily available in ITU-R 618-12 [13].

The proposed model is compared with some notable reduction factor models. These models are the Goddard [14], Lin [23], Moupouma [24], CETUC [25], Improved CETUC [26], ITU-R P.530-8 [27], Singapore [28], and DAH [29] models. The comparison is presented in Figs 5(a-e) at the specified path lengths for different frequencies.

At 12 GHz for example, the proposed reduction is similar to the Goddard model and generally

follows the same trend as other models, namely the DAH, ITU-R, Singapore, CETUC, Moupfouma and Lin models, as presented in Fig. 5a. The values for the proposed model are nearer to the Goddard and Improved CETUC models, although Improved CETUC model deviated totally at path length less than 2 km. The Goddard model was developed based on radar data as the proposed model. At high frequencies, especially at 35 GHz, the proposed

model shows a much lower reduction factor values up to about 15% as evident in Fig. 5e. This means that the proposed model will predict a lower attenuation value at higher frequencies. However, Moupfouma and DAH models are frequency dependent beside the proposed model. It has been shown in earlier sections that attenuation due to rain will increase with frequency.

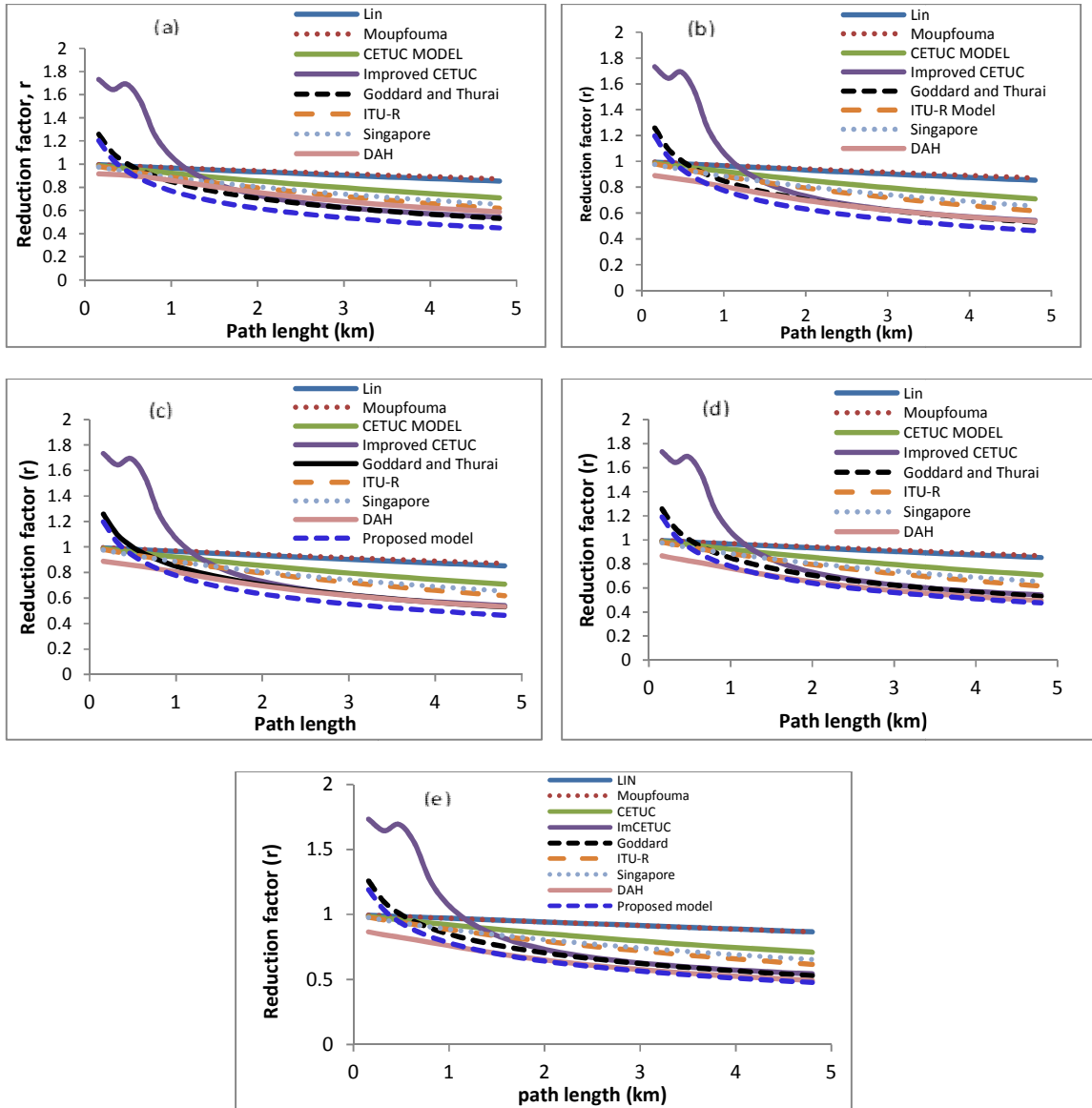


Fig. 5. Comparison of reduction factor models for different frequencies at (a) 12, (b) 16, (c) 20, (d) 30 and (e) 35 GHz

4.1 Testing the Proposed Model

Since measurement is available at 12.245 GHz based on the beacon data from the experimental site, the proposed model is tested with measured data alongside the specified notable models. Fig. 6 shows the cumulative distribution of the measured rain attenuation at 12.245 GHz beacon measurements compared with eight existing prediction models and the proposed model. From the figure, it is shown that the proposed model gives attenuation values that are a bit lower than the measured attenuation values especially at 0.05 to 0.001% availability time. DAH, CETUC and Moupfouma models underestimate the measured rain attenuation values at every percentage of time while ITU-R model underestimates at 1 to 0.01% and overestimate at $\leq 0.001\%$ availability time. The proposed model agrees reasonably well with measured values from low availability time up to 0.005 % time percentage. At time percentage above 0.005%, the proposed model deviated from the experimental values probability due to saturation of rainfall at high rain rate [11,30].

In all the time percentages considered, Lin and Singapore models continuously overestimate the

measured rain attenuation values. These models were developed using data from the temperate region. Improved CETUC and Goddard models showed similar pattern to the proposed model as well as the measured attenuation values, especially at lower frequency. The Improved CETUC was developed based on large and more accurate data based on ITU-R data that comprises some data from the tropics while the Goddard and Thurai model is a model developed from radar data. The proposed model can then be used to give an indication of attenuation due to rain, as it was developed using the local rain data.

The results of comparative metric measure of the models based on average relative error at 12 GHz is presented in Fig. 7 to test the suitability of the proposed model. The performance evaluation of the proposed model has been estimated based on the algorithm proposed in ITU-R recommendation P 311-15 [31]. Fig. 8 also presents the results of comparative test of the proposed model in terms of RMS error. The proposed model shows a significant improvement over the existing prediction models based on the lower rms and average relative error when compared with other models.

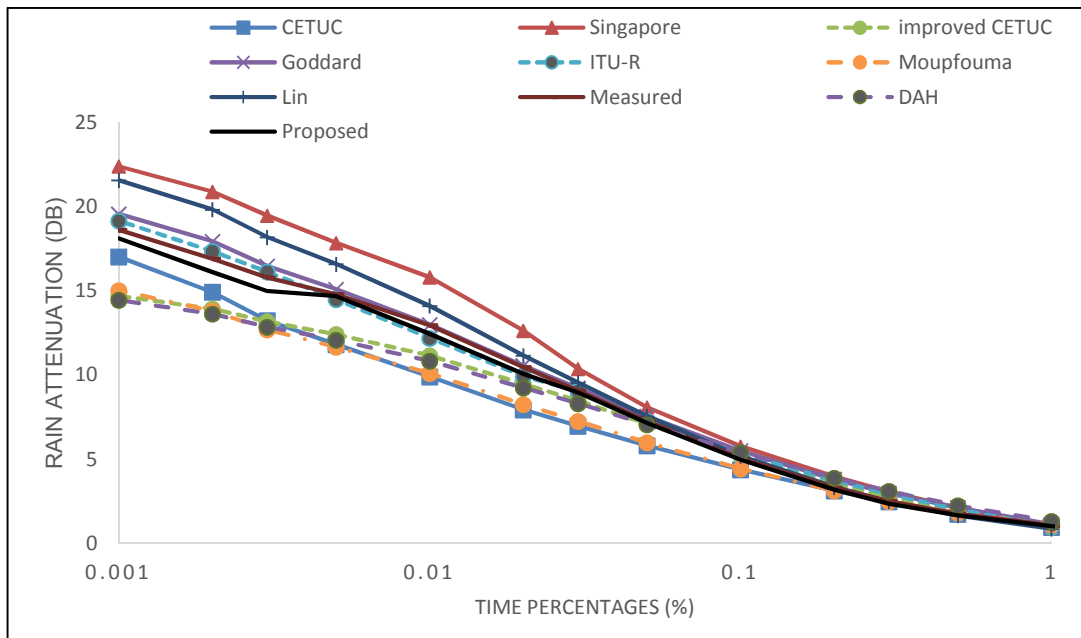


Fig. 6. Cumulative distribution of the measured rain attenuation compared with existing prediction models and the proposed model

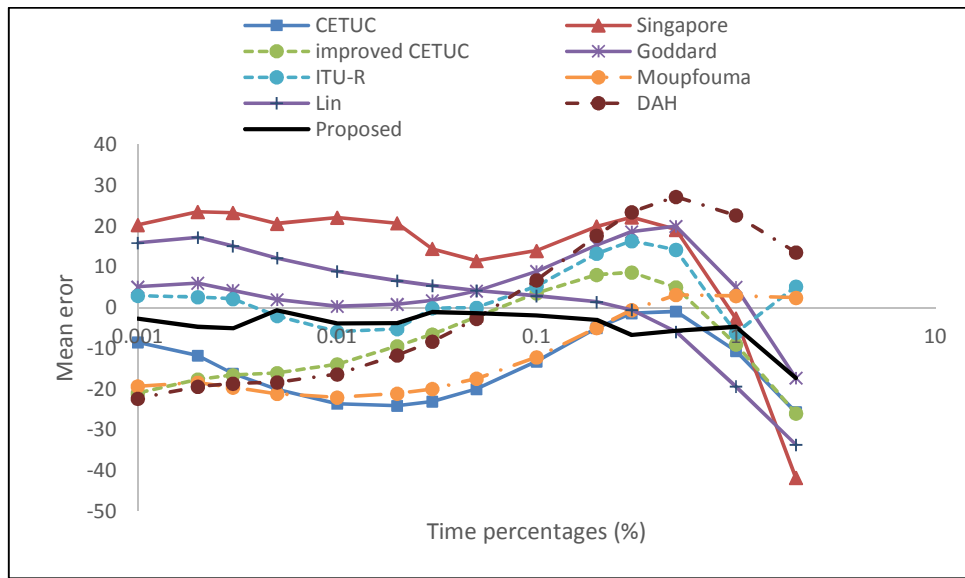


Fig. 7. Comparative metric measure of models based on average mean error at 12 GHz

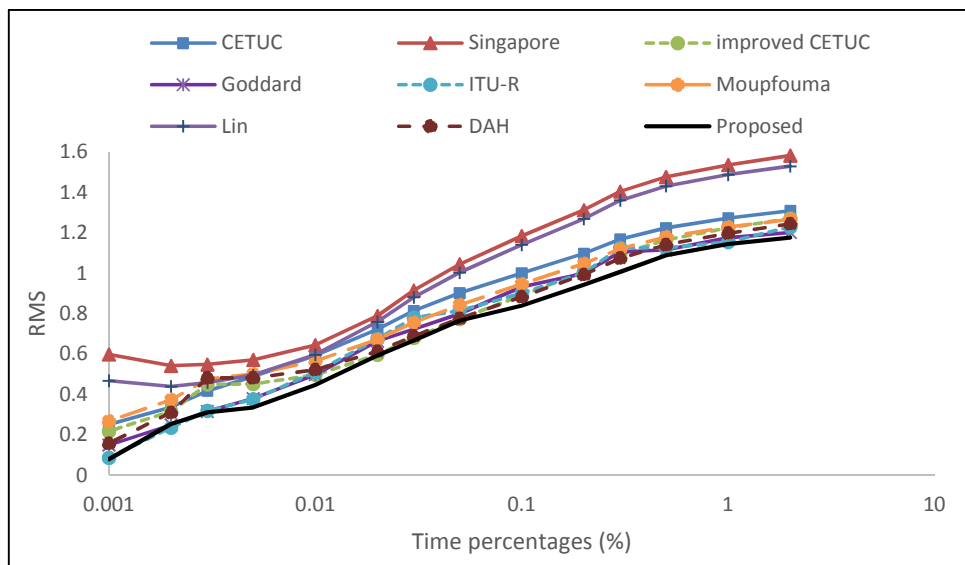


Fig. 8. Comparative metric measure of models based on rms at 12 GHz

5. CONCLUSION

In this study, an improved model for rain attenuation prediction is proposed based on radar data. Radar system exhibited wide coverage over a short period of time needed for modeling reduction factor. The reduction factor values decreases at higher frequencies with about 15% relative errors. The proposed model shows a significant improvement over the existing prediction models based on the lower *rms* and average relative error when compared

with other models. The empirical path reduction factor model is therefore proposed to be used for rain attenuation prediction for terrestrial and satellite applications in tropical region. It can also be applicable for other tropical region with similar rain rate pattern as that of Nigeria.

COMPETING INTERESTS

Authors have declared that no competing interests exist.

REFERENCES

1. McCormick KS. Rain attenuation measurements in South East Asia. Moscow, Dompars, Journal of Satellite, 1994;52(16):45 – 61.
2. Green HE. Propagation impairment on Ka-band Satcom link in tropical and equatorial region. 2004;46(2):31-45.
3. Adhikari A, Das S, Bhattacharya A, Maitra A. Improving rain attenuation estimation: modelling of effective path length using Ku band measurements at a tropical location. Progress in Electromagnetics Research B. 2011;34:173–186.
4. Ojo JS. Analysis of dynamical rain duration and return periods for terrestrial and satellite communication applications in a tropical climate. International Journal of Scientific & Engineering Research. 2016; 7(2):1306-1310.
5. Segal B. The influence of rain gauge integration time on measured rainfall-intensity distribution functions. Journal of Atmospheric and Oceanic Tech. 1986;3: 662-671.
6. Ajayi GO, Barbaliscia F. Prediction of attenuation due to rain: Characteristics of the 0°C isotherm in temperate and tropical climates. International Journal of Satellite Communication. 1990;8:187–196.
7. Crane RK. Rain attenuation models: Attenuation by clouds and rain. Propagation Handbook for Wireless Communication System, 225–280, CRC Press, U.S.A.; 2003.
8. Mandeep SJS, Hassan SIS, Ain MF, Ghani F, Kiyoshi I, Kenji T, Mitsuyoshi I. Earth-to-space improved model for rain attenuation prediction at ku-band. American Journal of Applied Sciences. 2006;3(8):1967-1969.
9. Ojo JS, Ajewole MO, Sarkar SK. Rain rate and rain attenuation prediction for satellite communication in Ku and Ka bands over Nigeria, Progress in Electromagnetics Research B. 2008;5:207–223.
10. Ippolito LJ. Satellite communication systems engineering: Atmospheric effects, Satellite link design, and system performance. John Wiley and Sons Ltd.; 2008.
11. Semire F. Abiola, Rosmiwati Mohd-Mokhtar, Widad Ismail Norizah Mohamad, Mandeep JS. Improved rain attenuation reduction factors for tropical region, proceeding of the 2013 IEEE International Conference on Space Science and Communication (Icon Space), 1-3 July Melaka, Malaysia; 2013.
12. ITU-R P.839-5: Rain Height for Prediction Methods, Int. Telecomm. Union, Geneva; 2015.
13. ITU-R P.618-12. Propagation data and prediction methods Requirement for the design of Earth-space. Telecommunication System; 2015.
14. Goddard JWF, Thurai M. Radar-derived path reduction factors for terrestrial systems, IEE 10th International Conference on Antenna and Propagation, 14-15 April 1997, Conference Publication No. 436,2.218-2.221.
15. Ayo AO, Ojo JS, Ajewole MO. Systematic variation of rain rate and radar reflectivity relations for micro wave applications in a tropical location. IOSR Journal of Applied Physics, 2015;7(6)Ver. I:23-29.
16. Durodola OM, Ojo JS, Ajewole MO. Performance of Ku-Band satellite signals received during rainy condition in two low latitude tropical locations of Nigeria, Adamawa State University Journal of Scientific Research. 2017;5(1):1-17.
17. Waldvogel A. The no jump of raindrop spectra. J. Atmos. Sci. 1974;31:1067-1078.
18. Peters G, Fischer B, Clemens M. Rain attenuation of radar echoes considering finite-range resolution and using drop size distributions. J. Atmos. Ocean. Technol. 2010; 27:829–842.
19. Marzuki H, Hashiguchi T, Kozu T, Shimomai Y, Shibagaki, Takahashi Y. Precipitation microstructure in different Madden-Julian oscillation phases over sumatra. Atmos. Res. 2016;168:121–138.
20. Peter G, Fischer B, Clemens N. Areal homogeneity of Z-R relations. Proceedings of ERA; 2006.
21. Bandera J, Papatsoris AD, Watson PA, Tozer TC, Tan J, Goddard JW. Vertical variation of reflectivity and specific attenuation in stratiform and convective rainstorms. Electron. Lett. 1999;35(7): 599-600.
22. Khamis NHH, Jafri Din, Tharek Abdul Rahman. Derivation of path reduction factor from the Malaysian meteorological radar data. 1st International Conference on Computers, Communications, & Signal Processing with Special Track on Biomedical Engineering, 2005. CCSP 2005.14-16 Nov; 2005. DOI: 10.1109/CCSP.2005.4977191

23. Lin SH. A method for calculating rain attenuation distributions on microwave paths. The Bell System Technical Journal. 1975;54(6):1051-1086.
24. Moupfouma F. Improvement of a rain attenuation prediction method for terrestrial microwave links. IEEE Trans on Antenna and Propagation. 1984;AP-32, Pt. H, no. 12:1368-1372.
25. Silva Mello LAR, Pontes MS, Souza RSL. Rain attenuation prediction for the design of site-diversity LEO/SMS Gateway configuration in the tropics. Proceedings Microwave and Optoelectronics Conference, 1997. 'Linking to the Next Century. 1997 SBMO/IEEE MTT-S International. 1997;2(2):11-14:729 – 733.
26. Garcia P, Selvo MLAR. Improved method for prediction of rain attenuation in terrestrial links. Electronic Letters. 2004; 40(11):683–684.
27. ITU-R P.530-8, Propagation Data and Prediction Methods required for the design of Terrestrial Line-of-Sight Systems. Int. Telecomm. Union, Geneva; 2004.
28. Ong JT, Timothy KI, Choo FBL, Carson WL. Effective rain height statistics for slant path attenuation prediction in Singapore. Electronics Letters, 30th March. 2000; 36(7):661-663.
29. Dissanayake, A., J. Allnutt, and F. Haidara, A prediction model that combines rain attenuation and other propagation impairments along earth-satellite paths, IEEE Trans. Antennas and Propag. 1997; 45:1546-1558.
30. Mandeep JS, Allnutt JE. Rain attenuation predictions at Ku-band in south East Asia countries. PIER. 2007;76:65-74.
31. ITU-R, Recommendation 311-15. Acquisition, presentation and analysis of data in studies of tropospheric propagation. ITU-R P Ser., Int. Telecomm. Union, Geneva; 2012.

© 2018 Ojo et al.; This is an Open Access article distributed under the terms of the Creative Commons Attribution License (<http://creativecommons.org/licenses/by/4.0>), which permits unrestricted use, distribution, and reproduction in any medium, provided the original work is properly cited.

Peer-review history:

*The peer review history for this paper can be accessed here:
<http://www.sciencedomain.org/review-history/24116>*